Electronic Supplementary Materials for "The sensory basis of schooling by intermittent swimming in the rummy-nose tetra (*Hemigrammus rhodostomus*)"

Amberle McKee, Alberto P Soto, Phoebe Chen, Matthew J McHenry

Department of Ecology and Evolutionary Biology
University of California, Irvine
321 Steinhaus Hall, Irvine, CA 92697

October 16, 2020

Methods

Animal care

We acquired adult rummy-nose tetra (*Hemmigrammus rhosostomus*) from the aquarium trade. The fish were held in a flow-through tank system (Aquatic Habitats, Apopka, FL, USA) in groups of $5-8$ fish in 3 L containers at 27° C on a 14:10 h light:dark cycle with daily feeding. Groups of 5 fish were transferred from the flow-through system into an experimental tank and allowed to acclimate ($>$ 30 min) prior to video recording. All rearing and experimental protocols were conducted with the approval of the Institutional Animal Care and Use Committee at the University of California, Irvine (IACUC Protocol #AUP-17-012).

Experimental setup and video recordings

We recorded the spontaneous swimming of fish in groups. The experimental tank included a cylindrical enclosure ($\varnothing \sim 67$ cm), a shallow water depth (13 cm), and a transparent acrylic floor (figure S1*a*). A large mirror positioned below the tank at a 45° angle allowed a high speed camera (FastCam SA2, Photron, San Diego, CA, USA) to record the behavior of the fish from below. Videos were captured using the Photron software (FASTCAM Viewer 3, Photron, with 28 mm lens) and stored on a RAID disk-array.

An arrangement of lights provided high-contrast images of the fish while exposing them to a variable intensity of visible light. The high-contrast illumination was provided by infrared LED lamps (IR Illuminator CM-IR200, Houston, Tx, USA; 850 nm) arranged at an oblique angle to a diffuser that was positioned above the tank (figure S1*a*). The LED lights were visible to the camera, but presumably not to the fish due to prior research [1] and our preliminary results, which indicated an inability to school under IR illumination. White light was provided by two lamps above the diffuser that were positioned close to, and directed toward, the ceiling of the room. These lamps were dimmable, each with a single LED bulb of modest maximum power (6 W) and showed no flicker when recorded with high-speed video at 1000 Hz. These bulbs provided a diffuse source of visible light that did not noticeably alter the contrast of the video images, which was dominated by the IR illumination. We measured the illuminance generated just above the experimental tank at variable dimmer settings using a light meter (L-758 Cine, Sekonic Corp., Tokyo, Japan) positioned at the tank's center, with the IR lights turned off.

In separate experiments, we recorded swimming over a long-duration or with high-speed video over a short duration. The long-duration recordings were recored at a time-lapse frame rate (0.5 frames s^{-1}, 2.5 ms exposure) that offered comprehensive kinematic measurements that viewed the entire cylindrical arena (~ 70 cm wide at 1536×1536 pixels), including interactions with the wall. The high-speed recordings (500 frames s^{-1}, 2 ms exposure) were focused on the center of the tank (~ 46 cm wide at 2048×2048 pixels) and permitted individual tracking and a detailed view of the spatial interactions between fish during schooling (figure S1*b*).

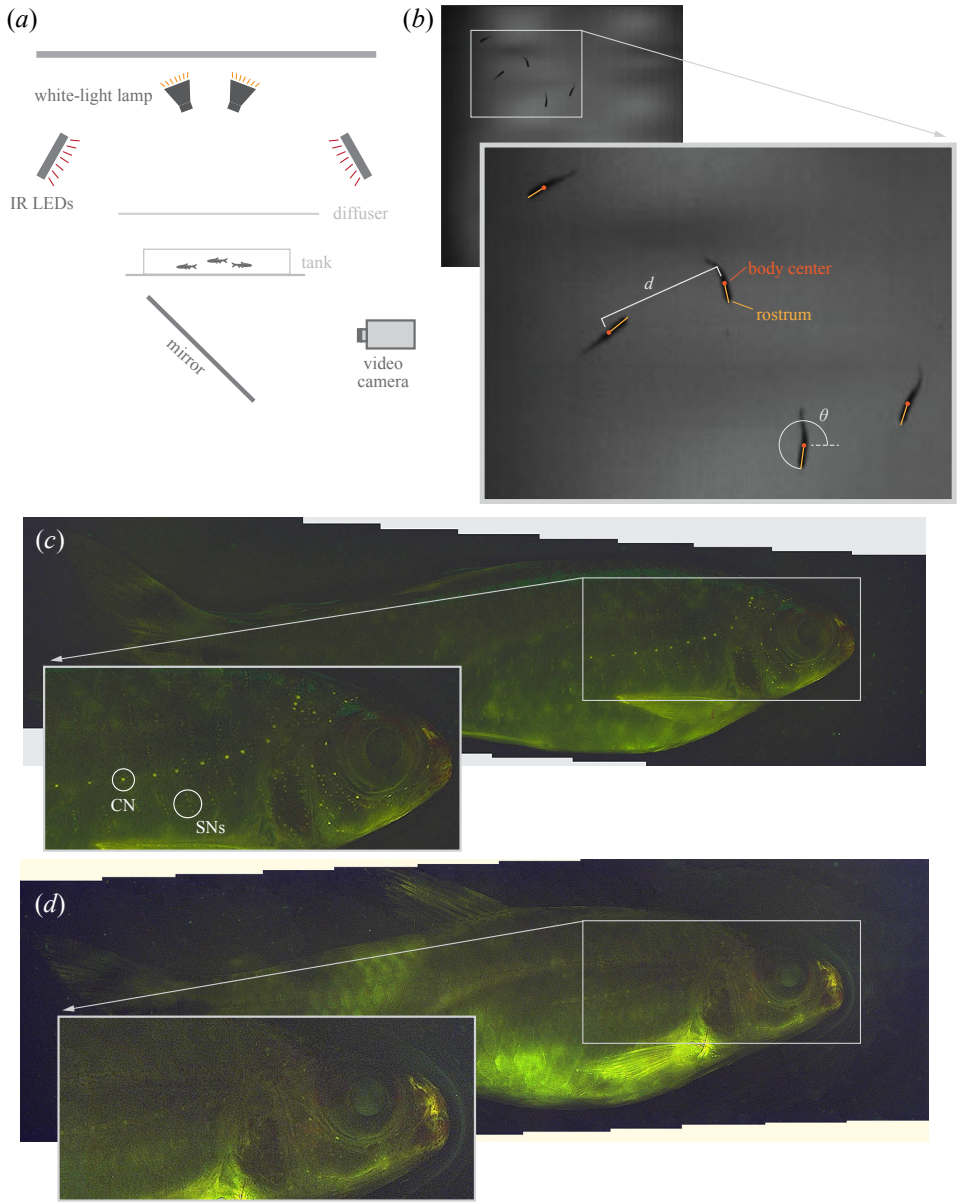

Figure S1: Kinematic measurements and experimental manipulation of the lateral line system. (a) Groups of 5 fish were recorded in an experimental tank that was illuminated with IR lights that were directed toward a diffuser, placed above the tank. Visible lights were directed toward the ceiling to provide reflected ambient illumination. (b) A video still of one of our high-speed recordings, which demonstrates the high contrast of the fish with the transmitted illumination provided by the IR lights. The inset highlights the automatic tracking of the positions of the body center and rostrum of each fish and illustrates measurements of the nearest-neighbor distance (d) and heading (θ). (c) The hair cells of the lateral line were visualized with fluorescent dye (DASPEI), with canal neuromasts (CN) appearing as relatively large circles and groups of superficial neuromasts (SNs) visible as circles that are more faint and smaller. (d) After exposure to an antibiotic (neomycin sulfate), the lateral line neuromasts were greatly attenuated in the intensity of the fluorescent dye.

Manipulation of lighting

We tested how schooling varies with light intensity with long-duration recordings. We recorded swimming for 30 min at each of 8 levels of illuminance (0 lx, 0.44 lx, 0.62 lx, 0.66 lx, 0.70 lx, 1.25 lx, 1.80 lx, and 8.15 lx). The order of these recordings was randomized and each recording was preceded by an acclimation period ($30 - 60$ min) at the illuminance level for the recording. A preliminary analysis of our results indicated an inability of the fish to school at close proximity with a high polarized orientation at low light intensities (< 1.50 lx). This prompted us to focus subsequent experiments that tested the role of flow sensing on experiments performed under bright light (8.15 lx) and dim light (1.80 lx) that was still sufficient for schooling.

Lateral line manipulation

We tested the role of flow sensing in schooling by experimental manipulation of the lateral-line system through exposure to a solution of neomycin sulfate (Fisher BioReagents,Fair Lawn, NJ, USA). This is a common procedure for inducing cell death among lateral line hair cells that does not affect the inner-ear hair cells used for hearing and balance [2]. Groups of fish were placed in a neomycin solution (0.27 g Neomycin sulfate in 300 ml fish water, pH = 7.2) for an extended period (2 hr) in the dark to avoid bleaching the light-sensitive neomycin. The fish were moved to a series of three fresh water rinses, each for 3 min. This protocol was developed by verifying its effects on lateral-line hair cells, as assessed by the fluorescent vital stain DASPEI (2-(4-(dumethylamino)styryl)-N-ethylpyridinium iodide; Invitrogen, Eugene, OR, USA). Fish were placed in a DASPEI solution (0.01 g DASPEI per 100ml water) for 15 min before 3 rinses. We then anesthetized the fish by placing them in a tricaine methanesulfonate (MS-222, Finquel, Argent Chemical Laboratories, Redmond, WA, USA) solution (4.2 ml concentrate MS-222 per 100ml water). We captured images of the entire length of the fish using a stereomicroscope (Zeiss Discovery V.20, Carl Zeiss, Thornwood, NY, USA) with a GPF filter set (450–490 nm), fluorescence illuminator (120 W Mercury Vapor Short Arc, X-Cite series 120q, Lumen Dynamics, Mississauga, ON, CA), and a camera (AxioCam HRc, Carl Zeiss). We allowed them to recover in a small holding tank of fresh fish water before returning them to a main tank. The photographs of DASPEI staining were later stitched together in Photoshop (v.21.0.3, Adobe, San Jose, CA USA).

Sample sizes

We replicated our experiments across multiple groups of 5 fish. We performed long-duration experiments at 8 levels of illuminance in 5 groups (i.e., 40 experiments with 25 fish). We tested the role of the lateral line system on long-duration kinematics in 4 treated groups and 4 control groups, each of which we tested for differences between dim (1.80 lx) and bright (8.15 lx) light (i.e., 32 experiments with 40 fish). Therefore, we performed a total of 72 long-duration experiments on 65 fish. Short-duration experiments were performed on 8 control groups and 8 treated groups. This

included the 40 fish used for the long-duration experiments and added an additional 40 fish (20 control in 4 groups, 20 treated in 4 groups). We performed 3 experiments under dim light and 6 under bright light for each of these groups. Due to the challenge of tracking individual fish over the entirety of an experiment, we successfully analyzed 141 out of the 192 short-duration experiments that were completed.

Automated acquisition of kinematics

We automated the acquisition of positional data of fish from our video with custom software. This process, and all other aspects of data analysis, was performed with scripting in MATLAB (R2018b, MathWorks, Natick, MA, USA) with the Computer Vision and Statistics Toolboxes. Our software calibrated the videos in a manner that corrected for radial lens distortion from video stills of a checkerboard placed at a variety of positions in the field of view (using the 'estimateCameraParameters' function). We differentiated the fish from the background first by calculating a single image from a video recording that appeared like an empty tank. This background image was determined by finding the 90% quantile value of each pixel across 100 frames that spanned each recording. Each video frame to be analyzed was inverted and we subtracted the pixel values of the inverted background image to yield an image of the video frame that isolated the moving fish, an image that we contrast-enhanced. The fish bodies were then identified by thresholding the processed images and filtering the resulting binary blobs by area. Occlusions, when one fish obstructs the view of another, were identified by an increase in blob area and frames that found fewer fish than the known number were rejected. The major axis of each blob served to identify the central orientation of the trunk and we evaluated the pixel values along the major axis and found that the anterior direction consistently included darker pixel values within a quarter of the body length from the centroid. We found the anterior margin of the rostrum by the spatial increase in pixel intensity in the anterior direction along the major axis. The posterior midline of the body was identified by first calculating the distance map of the blob. We then found the caudal peduncle as the highest pixel intensity in the posterior quadrant at the radial position from the body center at 0.4 times the major axis length.

Analysis of high-speed recordings

Our high-speed recordings provided the opportunity to track individuals over time and to glean detailed kinematics of swimming for each fish. This first required post-processing of the positional data where individuals across frames were initially identified as the closest centroid between consecutive frames. Occlusions and any other frames where the acquisition failed to find the known number of blobs presented gaps in temporal record for the positional data. These periods were neglected by our analysis if they occurred at the start or end of a recording. Otherwise, we used the closest last known coordinate to link individuals across gaps in the data and filled the gap by linear interpolation over the interval.

A preliminary analysis revealed that the duration of bouts of intermittent swimming could be identified by large accelerations and decelerations. We calculated the speed of individuals (v) from the discrete difference in centroid position and low-pass filtered the data with a moving average over 20 video frames. Our software identified these events from a discrete calculation of acceleration from our speed measurements, additionally filtered by a moving average of speed values across 30 frames. In an effort to characterize intermittent swimming kinematics, we examined relationships between the duration of swimming bouts, periods of rest between bouts, and both the change in speed and mean speed of swimming. In addition, we examined relationships in mean values of the change in speed, bout duration, and rest duration between focal fish and the others in a school.

These kinematic variables were compared by generalized linear mixed-effects models. We treated the school number (i.e., particular groups of 5 fish) as a random effect and the lighting and lateral line treatment were treated as fixed effects. For example, the mean change in speed over swimming bouts ($\overline{\Delta v}$) was modeled as a function of burst duration (T_{burst}) as follows:

$$\overline{\Delta v} \sim 1 + T_{\text{burst}} + \text{treat}_{\text{neo}} + \text{light}_{\text{dim}} + (1|\text{school}), \tag{S1}$$

where $\text{treat}_{\text{neo}}$ is a categorical variable (neomycin compared to control), $\text{light}_{\text{dim}}$ is another categorical variable (dim compared to bright), and school is the number of a particular school. Eqn. S1 is offered in Wilkinson notation [3]. We used generalized linear mixed-effects models to test the magnitude of turning and changes in speed during the burst phase. However, this analysis considered how changes in heading and speed varied with the position of neighboring fish and therefore permitted the opportunity for multiple measurements from a single experiment. We therefore categorized turns by the number of fish to the left or right of the focal fish and consequently treated the experiment number and fish number as additional random effects in our model. Our analysis of changes in speed considered the number of fish ahead and behind a focal fish, which allowed for multiple measurements that were also addressed by experiment number and fish number as random effects.

Analysis of long-duration recordings

Positional data provided the basis for measurements of kinematics from our long-duration recordings. Centroid tracking yielded sufficient measurements to satisfy the aim of the time-lapse recordings, which was to measure shoaling kinematics for groups, which did not require tracking individual fish over time. These measurements included the speed (V), nearest-neighbor distance (D), and polarization (ρ) of the group of fish. Speed was calculated as the discrete positional change in the mean coordinates of the group in each frame, divided by the change in time. The nearest neighbor at each time was identified as the minimum distance between each focal fish and the other fish in a school. As detailed in "Materials and methods", polarization offered a non-dimensional measure of the degree to which animals were oriented in the same direction, with possible values ranging from 0 to 1.

We compared mean values of kinematics over time between our experimental groups. These four groups were defined by bright and dim light and whether the fish had been treated with neomycin ('No lateral line') and the control. The comparison was performed as a two-way ANOVA with post-hoc comparisons performed by Fisher's least significant difference procedure [4, 5]. The post-hoc test included a consideration of an interactive effect between illuminance and flow sensing.

Results

Tables

Table S1: Generalized linear mixed-effects modeling for change in heading during the burst phase (figure 2*b*). CI, 95% confidence interval; SE, standard error; tStat, t-Statistic; DF, degrees of freedom; n_{toward}, number of fish toward turn; $\text{treat}_{\text{neo}}$, neomycin treatment; $\text{light}_{\text{dim}}$, dim light. Model in Wilkinson notation [3]: $|\Delta\theta| \sim 1 + n_{\text{toward}}$+ treat + light + (1|school) + (1|experiment) + (1|fish).

	coefficient						
variable	estimate	lower CI	upper CI	SE	tStat	DF	P
(intercept)	19.6	15.79	22.38	1.93	10.12	630	$<$ **0.001**
n_{toward}	1.95	0.93	2.97	0.52	3.74	630	$<$ **0.001**
$\text{treat}_{\text{neo}}$	-2.28	-5.98	1.41	1.88	-1.21	630	0.22
$\text{light}_{\text{dim}}$	-4.33	-7.30	-1.37	1.51	-2.87	630	**0.004**

Table S2: Generalized linear mixed-effects modeling for change in speed during the burst phase (figure S2). CI, 95% confidence interval; SE, standard error; tStat, t-Statistic; n_{ahead}, number of fish ahead; $\text{treat}_{\text{neo}}$, neomycin treatment; $\text{light}_{\text{dim}}$, dim light. Model in Wilkinson notation [3]: $|\Delta v| \sim 1 + n_{\text{ahead}}$+ treat + light + (1|school) + (1|experiment) + (1|fish).

	coefficient						
variable	estimate	lower CI	upper CI	SE	tStat	DF	P
(intercept)	5.31	4.25	6.37	0.54	9.88	629	$<$ **0.001**
n_{ahead}	0.21	0.01	0.41	0.10	2.08	629	**0.04**
$\text{treat}_{\text{neo}}$	-0.08	-1.32	1.17	0.64	-0.12	629	0.90
$\text{light}_{\text{dim}}$	-0.41	-0.29	1.11	0.36	1.16	629	0.25

Table S3: Generalized linear mixed-effects modeling for effects on speed, burst duration, and coast duration (figure S4). CI, 95% confidence interval; SE, standard error; tStat, t-Statistic; DF, degrees of freedom; $\overline{\Delta v}$, mean change in speed (cm s^{-1}); $\overline{v}$, mean speed (cm s^{-1}); T_{coast}, coast duration (s); T_{burst}, burst duration (s); $\text{treat}_{\text{neo}}$, neomycin treatment; $\text{light}_{\text{dim}}$, dim light. Models shown in Wilkinson notation [3].

	coefficient						
variable	estimate	lower CI	upper CI	SE	tStat	DF	P
$\overline{\Delta v} \sim 1 + T_{\text{burst}} +$ treat + light + (1|school)							
(intercept)	-1.69	-3.87	0.50	1.10	-1.53	123	0.13
T_{burst}	52.92	38.36	63.48	6.34	8.03	123	$<$ **0.001**
$\text{treat}_{\text{neo}}$	-0.14	-1.41	1.13	0.64	-0.22	123	0.82
$\text{light}_{\text{dim}}$	0.09	-0.86	1.04	0.48	0.19	123	0.85
$\overline{v} \sim 1 + T_{\text{burst}} +$ treat + light + (1|school)							
(intercept)	4.11	1.69	6.53	1.22	3.36	123	**0.001**
T_{burst}	9.69	-2.26	21.63	6.03	1.61	123	0.11
$\text{treat}_{\text{neo}}$	-0.77	-2.92	1.38	1.09	-0.71	123	0.48
$\text{light}_{\text{dim}}$	2.18	-1.29	3.08	0.45	4.82	123	$<$**0.001**
$T_{\text{coast}} \sim 1 + T_{\text{burst}} +$ treat + light + (1|school)							
(intercept)	0.79	0.59	0.99	0.10	7.80	121	$<$**0.001**
T_{burst}	-1.03	-2.15	0.08	0.56	-1.84	121	0.07
$\text{treat}_{\text{neo}}$	0.07	-0.06	0.20	0.07	1.03	121	0.31
$\text{light}_{\text{dim}}$	-0.17	-0.25	-0.08	0.04	-3.86	121	$<$**0.001**
$\overline{v} \sim 1 + T_{\text{coast}} +$ treat + light + (1|school)							
(intercept)	8.31	6.58	10.04	0.88	9.49	124	$<$**0.001**
T_{coast}	-4.23	-6.01	-2.44	0.90	-4.69	124	$<$**0.001**
$\text{treat}_{\text{neo}}$	-0.49	-2.25	1.28	0.89	-0.54	124	0.59
$\text{light}_{\text{dim}}$	1.29	-0.39	2.19	0.45	2.85	124	**0.005**

Table S4: Generalized linear mixed-effects modeling for relationships in kinematics between focal fish and other fish (figure S5). CI, 95% confidence interval; SE, standard error; tStat, t-Statistic; DF, degrees of freedom; $\overline{\Delta v}$, mean change in speed (cm s^{-1}); T_{coast}, coast duration (s); T_{burst}, burst duration (s); $\text{treat}_{\text{neo}}$, neomycin treatment; $\text{light}_{\text{dim}}$, dim light. Models shown in Wilkinson notation [3].

	coefficient						
variable	estimate	lower CI	upper CI	SE	tStat	DF	P
$\overline{\Delta v}_{\text{focal}} \sim 1 + \overline{\Delta v}_{\text{other}}$+ treat + light + (1|school)							
(intercept)	1.62	0.35	2.89	0.64	2.53	126	**0.01**
$\overline{\Delta v}_{\text{other}}$	0.67	0.49	0.85	0.09	7.53	126	$<$ **0.001**
$\text{treat}_{\text{neo}}$	-0.14	-1.04	0.76	0.45	-0.31	126	0.76
$\text{light}_{\text{dim}}$	0.78	-0.02	1.57	0.40	1.93	126	**0.05**
$T_{\text{coast,focal}} \sim 1 + T_{\text{coast,other}}$+ treat + light + (1|school)							
(intercept)	0.32	0.09	0.55	0.12	2.76	119	**0.006**
$T_{\text{coast,other}}$	0.53	0.19	0.87	0.17	3.07	119	**0.002**
$\text{treat}_{\text{neo}}$	0.01	-0.13	0.14	0.07	0.10	119	0.92
$\text{light}_{\text{dim}}$	-0.05	-0.20	0.10	0.07	-0.67	119	0.50
$T_{\text{burst,focal}} \sim 1 + T_{\text{burst,other}}$+ treat + light + (1|school)							
(intercept)	0.08	0.05	0.12	0.02	4.45	121	$<$**0.001**
$T_{\text{burst,other}}$	0.44	0.21	0.67	0.11	3.85	121	$<$**0.001**
$\text{treat}_{\text{neo}}$	0.002	-0.010	0.013	0.006	0.30	121	0.77
$\text{light}_{\text{dim}}$	0.010	0.001	0.023	0.005	2.18	121	0.03

Additional figures

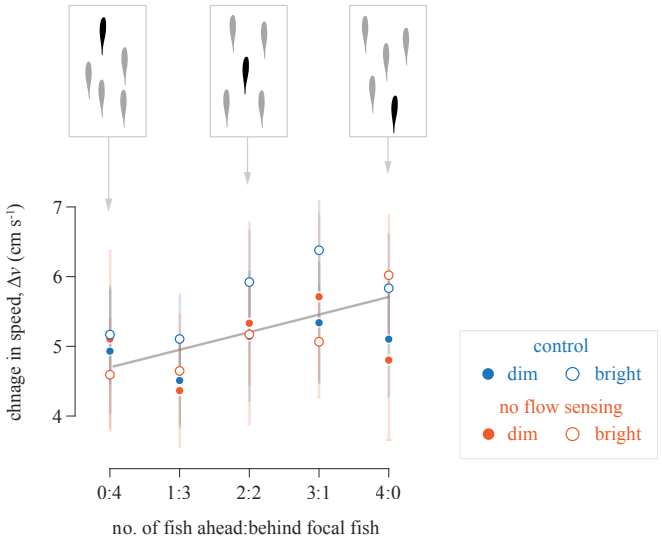

Figure S2: Change in speed during the burst phase, relative to the number of fish ahead and behind the focal fish. Measurements are shown for four neomycin-treated (i.e., 'no flow sensing', red, $n = 8$) and control (blue, $n = 8$) groups under dim (1.80 lx, filled circles) and bright (8.15 lx, open circles) light for 141 experiments, with analysis of all 5 individuals from each group. Mean values are plotted with 95% confidence intervals that assume a normal distribution. The line shows the linear relationship with respect to the position of neighboring fish ($r^2 = 0.60$). Our generalized linear mixed-effects model found no significant effects of illuminance and the lateral-line treatment (table S2).

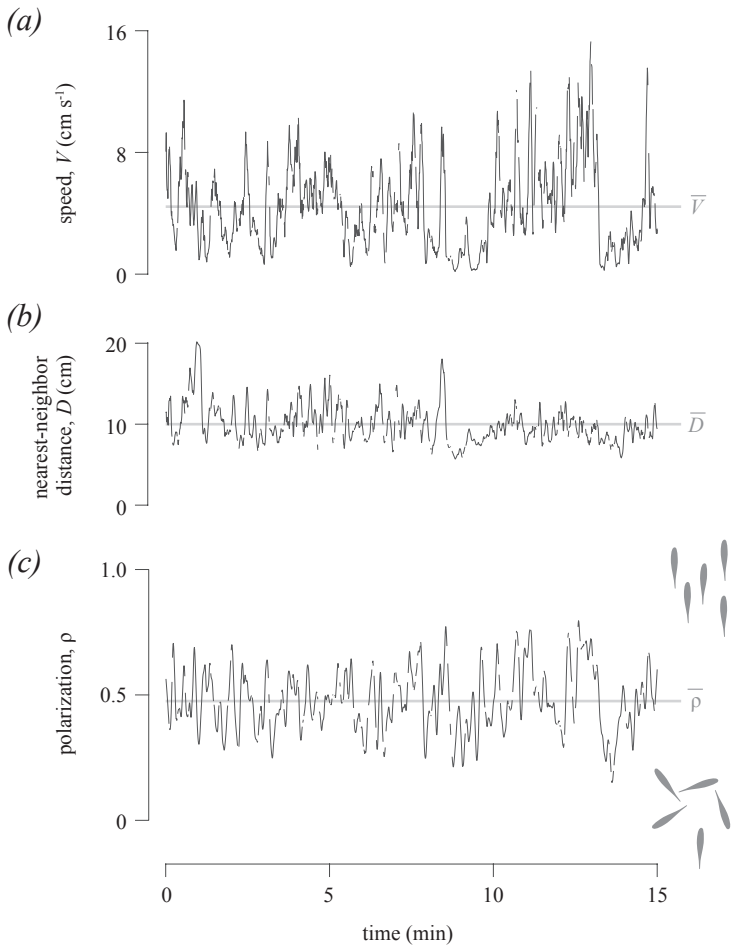

Figure S3: Representative long-duration kinematic measurements, as recorded by time-lapse (0.5 frames s^{-1}) videography. (*a–c*) Schooling kinematics for a group of 5 fish, as measured by mean values among the members for the (*a*) speed, (*b*) nearest-neighbor distance, and (*c*) polarization for swimming at a fixed light intensity (8.15 lx). Speed and distance were calculated as the mean value at each time among all individuals. Polarization was calculated at each time by integration among the group members (equation 2.1) and the schematic to the right illustrates two groups of fish at extreme values of polarization. The mean values (gray horizontal line) are highlighted in each panel. These plots show half of the duration of a full (30 min) experiment to visualize the temporal variation. Gaps in the traces correspond to frames where occlusions or other failures in tracking occurred.

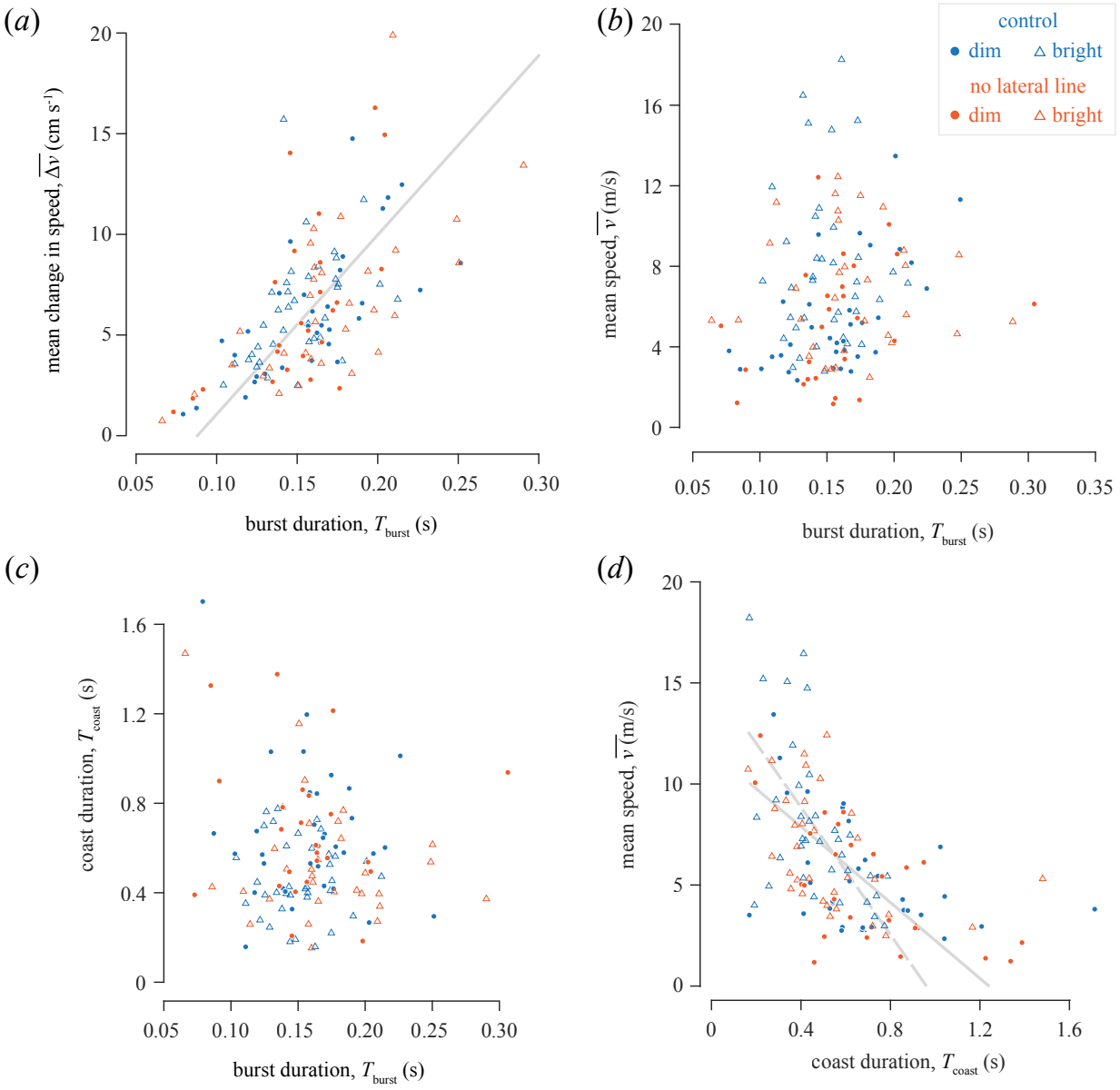

Figure S4: The change in speed during a burst of swimming ($\overline{\Delta v}$) and the time-averaged mean speed ($\overline{v}$) are shown with respect to the duration of swimming bursts (T_{burst}) and the periods of coasting (T_{coast}) between bouts for 127 experiments conducted for control ($n = 8$) and neomycin-treated ($n = 8$) groups (5 fish per group). Each symbol represents the mean value for 3 or more bouts of swimming among a unique group of 5 fish in an individual experiment. The legend in the upper-right differentiates the symbols by the 4 experimental treatment groups. Trend lines are shown for the significant factors, according to our generalized linear mixed-effects model (table S3). (*a*) Variation in the mean change in speed is positively related to the bout duration ($r^2 = 0.34$). No such relationships were found between (*b*) bout duration and mean speed ($r^2 = 0.03$) or (*c*) bout duration and rest duration ($r^2 = 0.02$). However, (*d*) a negative relationship was found between rest duration and mean speed for experiments under dim light (1.80 lx, solid line, $r^2 = 0.26$) and bright light (8.15 lx, dashed line, $r^2 = 0.26$).

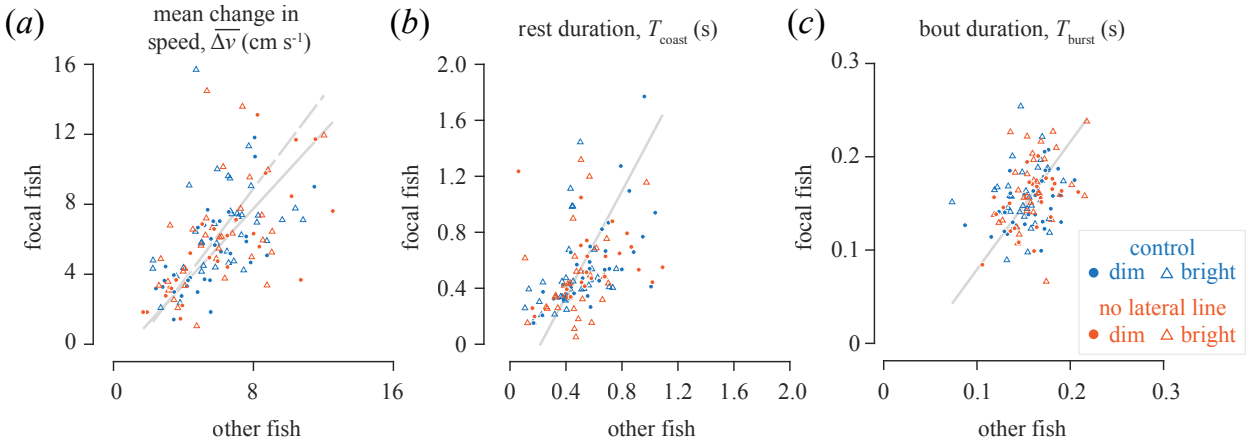

Figure S5: Relationship in kinematic parameters between focal fish and the other members of a school. Each symbol represents the mean value for 3 or more bouts of swimming among a unique group of 5 fish in an individual experiment ($n = 130$). The legend (right side) differentiates the symbols by the 4 experimental treatment groups. (a) Variation in speed by focal fish is partially predicted by the speed of others for experiments under dim light (1.80 lx, solid line, $r^2 = 0.52$) and bright light (8.15 lx, dashed line, $r^2 = 0.18$). Less of the variation in (b) rest duration ($r^2 = 0.09$), or (c) the bout duration ($r^2 = 0.10$) of focal fish may be predicted by those variables in neighboring fish. See table S4 for the results of generalized linear mixed-effects modeling.

Bibliography

[1] Silver, P., 1973 Photopic spectral sensitivity of the neon tetra *Paracheirodon innesi* (Myers) found by the use of a dorsal light reaction. *Vision Res.* **14**, 329–334.

[2] Harris, J. A., Cheng, A. G., Cunningham, L. L. & G, M., 2003 Neomycin-induced hair cell death and rapid regeneration in the laterl line of zebrafish *Danio rerio*. *J. Assoc. Res. Otolaryn.* **4**, 219–234. (doi:10.1002/wdev.160).

[3] Wilkinson, G. N. & Rogers, C. E., 1973 Symbolic description of factorial models for analysis of variance. *J. Royal Stat. Soc.* **22**, 392–399.

[4] Milliken, G. A. & Johnson, D. E., 1992 *Analysis of Messy Data. Volume I: Designed Experiments.* Boca Raton, FL: Chapman & Hall/CRC Press.

[5] Hochberg, Y. & Tamhane, A. C., 1987 *Multiple Comparison Procedures.* Hoboken, NJ: John Wiley & Sons, Ltd.